On–axis Instrumental Polarization Calibration for Linear Feeds

W. D. Cotton, August 7, 2015

***Abstract*—Various instrumental and atmospheric effects corrupt the response of an interferometer to polarized signals. In the case of high dynamic range imaging, uncorrected, these effects can also degrade the total intensity image. These effects must be estimated and removed in order to produce images of the polarized emission, or high dynamic range total intensity images. This memo describes the implementation in Obit of the feed ellipticity–orientation modeling and correction for arrays with linearly polarized feeds. Examples are given using data from the KAT-7 and ALMA arrays.**

***Index Terms*—interferometry, polarization, calibration**

I. Introduction

RADIO interferometric imaging of polarized celestial emission provides a powerful probe of various physical processes as well as the propagation through intervening media. Instrumental and atmospheric effects corrupt the response of an interferometer to polarized signals. In particular, the array detectors do not respond to precisely the intended polarization state which leads to a spurious polarized response.

Detectors sensitive to the electric field of the incoming wave, as used in radio heterodyne systems, respond to a single polarization state; in order to fully measure the polarization of the wave, detectors measuring orthogonal polarization states are needed. In the correlation process, all four products of the two states at each antenna are produced. The most commonly used systems are right- and left-hand circular polarization and orthogonal linear polarizations. In practice, the detected polarizations are never precisely the desired ones. The exact polarization states detected must be determined in order to transform the measured visibilities into the corrected form.

This memo describes an implementation in the Obit package [1] [1] of the nonlinear ellipticity–orientation model for arrays using alt-az mounted antennas and using detectors (AKA "feeds") sensitive to orthogonal linear polarizations. The result of the application of the calibration derived is the observed data corrected and transformed into a circular basis. Calibration of arrays with circular feeds is discussed in [2]. The development here follows that of [3].

II. Interferometric Polarimetry

An arbitrary electromagnetic wave can be described as elliptically polarized, circular and linear polarization are extreme cases. One way of modeling the polarization state to which a detector responds is the ellipticity and orientation of the ellipse to which the detector responds. An alternate, and popular approach is to model the response as the desired state plus a fraction of the orthogonal state. The fraction of the orthogonal state is referred to as the "leakage term". This model has the advantage that it can be linearized allowing for faster fitting. See [4][5][6] for more detailed descriptions of the response to polarized radiation.

Much traditional radio interferometric software at the NRAO uses data from arrays using circular feeds. Therefore, it is convenient to have the transformation of observed to calibrated data to also transform the visibilities into a circular basis, i.e. what would have been observed with circular feeds.

A. Effects of prior calibration

Discussions of instrumental polarization such as those given in [4] generally do not include the effects of prior calibration on the data. The common practice is to calibrate the two parallel polarization systems of visibilities independently.

Since interferometers only measure differences of the phase of a wavefront between pairs of antennas, the absolute phase is undetermined and phases are referred to that at a reference antenna whose phase (and delay) has been arbitrarily set to zero. This allows for an arbitrary phase and delay offset between the independent polarization systems. See [7] for a discussion of correcting these offsets.

B. Response by Linear Feeds

For an interferometer with perfectly linear feeds observing an unresolved, partially polarized source and forming all four correlation products the expected visibility [XX,XY,YX,YY] is given by [8]:

$$\begin{aligned}\mathbf{S_L} = [&ipol + qpol\ cos(2\psi) + upol\ sin(2\psi),\\ &- qpol\ sin(2\psi) + upol\ cos(2\psi) + j\ vpol,\\ &- qpol\ sin(2\psi) + upol\ cos(2\psi) - j\ vpol,\\ &ipol - qpol\ cos(2\psi) - upol\ sin(2\psi)]\end{aligned}$$

where $ipol$, $qpol$, $upol$ and $vpol$ are the Stokes' I, Q, U and V of the source and j is $\sqrt{-1}$. ψ is the angle between the "X" feed and the meridian measured from north towards east. This is a combination of the orientation of the feed wrt the antenna (ϕ) and the orientation of the antenna wrt the sky (χ). The "Y" is then presumed to be orientated by a further 90° from the X feed. χ is the parallactic angle given by:

$$\chi \ = \ \tan^{-1}\Big(\frac{\cos\lambda\ \sin\ h}{\sin\ \lambda\ \cos\ \delta\ -\ \cos\ \lambda\ \sin\ \delta\ \cos\ h}\Big) \quad (1)$$

National Radio Astronomy Observatory, 520 Edgemont Rd., Charlottesville, VA, 22903 USA email: bcotton@nrao.edu

[1]http://www.cv.nrao.edu/∼bcotton/Obit.html

where δ is the source declination, λ is the latitude of the antenna and h is the hour angle of the source. For interferometers using linear feeds, Stokes Q and U contribute to all four correlation products.

For an interferometer using perfect circular feeds, the equivalent visibility [RR,RL,LR,LL] is[4]:

$$\mathbf{S_C} = [ipol+vpol,\ qpol+j\ upol,\ qpol-j\ upol,\ ipol-vpol] \quad (2)$$

In this case, the cross–polarized components (RL, LR) give the linearly polarized response to the source without a dependency on the parallactic angle. In practice, the feeds are never precisely that desired and some fraction of the one polarization leaks into the other giving rise to a spurious "instrumental polarization".

The model used here describes each feed in terms of its ellipticity, θ and the the orientation of this ellipse, ϕ. The response of a given interferometer is given by a Muller matrix (4×4 complex matrix). This matrix multiplied by the true source polarization vector corrects for the effect of parallactic angle and residual calibration errors gives the model value of the visibilities. The strategy followed here is to determine the Muller matrices needed to transform the observed data to a circular basis while correcting for instrumental polarization.

The Muller matrix for a given baseline is the outer product of the Jones matrix for the first antenna times the conjugate of that for the second. A Jones matrix including residual calibration can be constructed for each antenna:

$$\mathbf{J} = \begin{vmatrix} g_X cos(\frac{\pi}{4}+\theta_X)e^{-j(\phi_X)} & g_X sin(\frac{\pi}{4}+\theta_X)e^{j(\phi_X)} \\ g_Y sin(\frac{\pi}{4}-\theta_Y)e^{j(\phi_Y)} & g_Y cos(\frac{\pi}{4}-\theta_Y)e^{-j(\phi_Y)} \end{vmatrix}$$

where g_X and g_Y are corrections to the gains of the X and Y feeds resulting from the parallel hand calibration.

The Muller matrix, M_{ik}, for baseline i-k is then the outer product of $\mathbf{J}_i$ and $\mathbf{J}_k^*$.

$$\mathbf{M}_{ik} \ = \ \mathbf{J}_i \ \otimes \mathbf{J}_k^*$$

Computation of the Muller matrix is described in more detail in the Appendix.

Applying a rotation for the parallactic angle, the predicted correlation vector is then

$$\mathbf{V}_{model\,ik} \ = \ \mathbf{M}_{ik}\ \mathbf{S_C} \begin{vmatrix} \Delta\chi_{ik}^* & 0 & 0 & 0 \\ 0 & \Sigma\chi_{ik}^* & 0 & 0 \\ 0 & 0 & \Sigma\chi_{ik} & 0 \\ 0 & 0 & 0 & \Delta\chi_{ik} \end{vmatrix} \quad (3)$$

where

$$\mathbf{V}^T_{model\,ik} \ = \ [XX_{ik},\ XY_{ik},\ YX_{ik},\ YY_{ik}].$$

and

$$\Delta\chi_{ik} = e^{j(\chi_i - \chi_k)}$$
$$\Sigma\chi_{ik} = e^{j(\chi_i + \chi_k)}$$

C. Source and instrumental polarization

In the general case, the polarization of the calibrator is unknown and must be solved for jointly with the instrumental polarization. For arrays with alt-az antenna mounts, the variation in the parallactic angle at which a calibrator is observed introduces a different effect on the source and instrumental polarization. Since the instrumental polarization is introduced in the frame of the antenna, it is constant with parallactic angle. To separate the two contributions to the polarized response requires that at least one calibrator be observed over a sufficient range of parallactic angle to separate the two effects. How much is enough depends on the SNR but generally a radian or more is desirable. For a calibrator of known polarization, including none, any distribution of parallactic angle is usable. A calibrator of known polarization angle is required to constrain the feed orientation.

D. Absolute v. Relative Calibration

To first order, the equations describing the polarized response for a short baseline interferometer are degenerate in that there are more parameters than independent measurements. This degeneracy is broken by the higher order terms if they are large enough. In practice, feeds with linear polarization frequently have low polarization imperfections and other constraints may be needed. These may be that a given (reference) antenna is defined to be "perfect" and its parameters fixed or that an average over the array of some parameter is "perfect".

III. Solutions for Model Parameters

The parameters of the model described in Section II-B can be fitted to a data set using any of a number of techniques. In the following two such techniques are explored.

A. Relaxation fitting

Following the method of [2] the first technique considered is a relaxation technique in which corrections are cyclically made to each model parameter being fitted by determining the effect of that parameter on the χ^2. The χ^2 of the fit is defined as

$$\chi^2 = \sum_{i=0}^{n} (model_i - obs_i)^2/\sigma_i^2$$

where $model_i$ is the model value for observation i (real or imaginary part of visibility), obs_i is the observation for i and σ_i^2 is the variance of the amplitude of observation i. The model values are components of the vector V_{model} given by Eq. 3. For each parameter, P, in each iteration, n, the revised value is given by:

$$P_{n+1} = P_n \ + \ tan^{-1}\Big(\frac{\frac{\partial\chi^2}{\partial P}}{\frac{\partial^2\chi^2}{\partial P^2}}\Big)$$

subject to the constrain that the corrected value, P_{n+1}, leads to a decrease in χ^2. Should this not be the case, the correction is reduced in magnitude until the χ^2 decreases. Note: the evaluation of χ^2 only need consider data which depend on the given parameter. The various partial derivatives are given in the appendix. In the following, this is referred to as the "fast" technique.

B. General nonlinear least squares

Most scientific software packages provide a generalized nonlinear least squares facility such as the Levenberg-Marquardt least squares technique. These can provide robust solutions as well as an error analysis but can be expensive to compute. An initial estimate of the parameters using the relaxation technique can reduce the total computing cost. These generalised nonlinear least squares packages generally need the derivatives of either the χ^2 or the model wrt the various parameters; these derivatives are given in the appendix.

IV. Correcting Observed Visibilities

Once the model parameters describing the instrumental polarization are known, they can be used to remove the instrumental effects from the data. The corrected visibility vector V_{corr} can be obtained from the observed visibility vector V_{obs} by

$$\mathbf{V'}_{cor} \;=\; \mathbf{M}^{-1}\;\mathbf{V}_{obs} \tag{4}$$

where M^{-1} is the inverse of the Muller matrix. A useful property of the outer product is that the the outer product of the inverses of two Jones matrices is the inverse of the outer product of the Jones matrices themselves. The inverse of a 2×2 matrix given by:

$$\mathbf{J} = \begin{vmatrix} a & b \\ c & d \end{vmatrix}$$

is

$$\mathbf{J}^{-1} = \frac{1}{ad - bc}\begin{vmatrix} d & -b \\ -c & a \end{vmatrix}$$

In the implementation described here, the multiplication by the inverse Muller matrix will transform the observed [XX,XY,YX,YY] visibilities into corrected [RR,RL,LR,LL] visibilities. These then need correction for the parallactic angle:

$$\mathbf{V}_{cor} \;=\; \begin{vmatrix} \Delta\chi_{ik} & 0 & 0 & 0 \\ 0 & \Sigma\chi_{ik} & 0 & 0 \\ 0 & 0 & \Sigma\chi^*_{ik} & 0 \\ 0 & 0 & 0 & \Delta\chi^*_{ik} \end{vmatrix} \mathbf{V'}_{cor} \tag{5}$$

A. Y/X Gain

The parallel hand calibration is generally done assuming unpolarized calibrators. As was shown in Section II-B, actual calibrator polarization will have an additive effect of the parallel hand visibilities with opposite signs and which vary with parallactic angle. If an unpolarized source is included in the data, it can be incorporated in the the parallel han calibration to fix the relative gains in the calibration process and then constrain further calibrations to average the paralle hands and thus cancelling the effects of calibrator polarization.

Lacking an unpolarized calibrator, a segment of data on a polarized calibrator over which the parallactic angle has minimal change can be used to constrain the X/Y gains followed by averaging the parallel hand data before calibration. This will leave an error in the Y/X gain ratio determined by the calibrator polarization and the parallectic angle of the calibration. Solving for the Y/X gain ratio can be included in the calibration fitting.

V. Obit implementation: PCal

Implemention of this calibration technique in Obit is in the task PCal which uses the software class ObitPolnCalFit. Multiple calibrators may be included in the solution. Calibration is per channel or sliding window of channels. Fitted feed parameters are stored in an AIPS PD table with the "Real" part being the ellipticity and the "Imaginary" being orientation. The table is labeled as type "ORI-ELP".

Fitting always uses the "fast" Relaxation method optionally followed by a Levenberg-Marquardt least squares using the GSL package nonlinear fitter. The initial value of the parameters are for perfect feeds for the first channel fitted and the results of the previous channel in subsequent fittings.

The parameters to PCal allow specifying the source polarizations for some subset of the calibrators in terms of the fractional polarization, the EVPA$\times 2$ and the rotation measure. In this case, the X-Y phase offset in the data should also be solved for and the results stored in the AIPS PD table as well as an AIPS BP table.

Application of instrumental polarization corrections to the data computes the inverse Muller matrix from the outer product of the inverse of the Jones matrices. The antenna Jones matrices are derived as described in Section II-B.

A. Feed orientations

In order to constrain the orientations of feeds, observations of a source of known polarization angle is needed. Fortunately, for feeds sensitive to linear polarization the orientation of the feed can be readily measured. If the feed orientation are known to sufficient accuracy (and given in the Antenna table) they need not be fitted. Obit/PCal allow either fitting for the feed orientation or leaving it at the nominal value.

B. X-Y phase difference

Typically, the calibration of tha parallel hand gains is done independently leaving an arbitrary difference in phase and group delay between the two systems. An initial estimate of the delay difference can be obtained and removed using Obit task RLDly [7]. Residual X-Y phase differences can be estimated in the fitting if one or more of the calibrators is polarized although its state need not be previously known. These phase differences are included in the output bandpass (AIPS BP) table.

C. Y/X Gain

As described in Section IV-A the Y/X gain ratio may not be properly determined by the parallel hand calibration and can be included in the calibration fitting. In PCal the relative cans can be determined in each channel or block of channels fitted and can be incorporated into the output bandpass table.

D. Stokes V

The value of Stokes' V can be left at 0 or fitted on a calibrator by calibrator basis.

TABLE I
Calibrator polarization

Source	Day	I Jy/bm	frac. lin. pol	EVPA °	frac. cir. pol
3C286	1	14.6	0.094	29.6	6.6e-5
3C138	1	8.6	0.072	-20.0	0.0017
B1934-638	1	14.5	0.0001	133	-0.0006
ph cal	1	0.90	0.037	-78.8	0.0003
3C286	2	14.1	0.096	29.5	8.9e-6
3C138	2	8.5	0.074	-21.5	0.0010
B1934-638	2	14.5	0.0003	-1.5	0.0007
ph cal	2	0.90	0.038	-78.0	0.0003
3C286	3	13.4	0.100	29.5	0.0005
B1934-638	3	14.0	0.001	-13.0	-1.8e-5
quasar	3	2.71	0.033	54.3	0.0008

E. Absolute or Relative Calibration

There are several options for relative v. absolute calibration and these are controlled by parameter refAnt. If refAnt is specified as zero, then no additional constraints are imposed and an "absolute" calibration is attempted. If refAnt is greater than 0, then it indicates an antenna for which the XPol ellipticity is fixed to zero (perfect feed). If refAnt is -1 then the average of all ellipticities is forced to zero. The latter option seems most effective when Stokes V is desired.

VI. EXAMPLES WITH KAT-7 DATA

The implemention in Obit was tested using data from the KAT-7 (MeerKAT prototype) array in South Africa. This array used linear feeds oriented vertically and horizontally and operates in L Band. Data were calibrated using the strong, very weakly polarized source B1934-638 and other calibrators were self calibrated averaging the parallel hand data to avoid introducing artifacts from the calibrator's polarization. All data sets included B1934-638 and 3C286 and the latter was used in RLDly to correct the cross polarized delay. Instrumental polarization calibration used fixed polarization models for B1934-638 (zero linear polarization) and 3C286 (0.095 fractional linear polarization at 1.3 GHz and 0.098 at 1.8 GHz at EVPA=33°). After calibration, the data were imaged and as all sources were unresolved, the value in the Stokes I, Q, U and V images at the location of the calibrator were used for evaluation. Polarization results are given in Table I and the associated image's RMSes in Table II.

Two datasets included both 3C138 and 3C286 as polarization calibrators and were identically scheduled which allows comparisons of repeatability. These were observed at 1.3 GHz allowing the posibility of variable ionospheric Faraday rotation. The results are summarized in Tables I and II as days 1 and 2.

A third dataset included a deep integration of a polarized quasar. This dataset was calibrated and imaged as were the previous tests and the images in various Stokes parameters are shown in Figure 1 and statistical measures in Tables I and II.

VII. EXAMPLE WITH ALMA DATA

ALMA polarization comissioning data was used to derive polarized images of the well known calibrator 3C286 at 230 GHz. Data consisted of four 2 GHz bands with all correlation products recorded. The observations included calibrators 3C279, J1337-1257, and J131029+322051 for bandpass, polarization and phase calibration. ALMA uses linearly polarized feeds at 45° to either side of vertical. The calibration proceeded as follows:

1) 3C279 and J1337-1257 were used for the parallel hand group delay calibration.
2) The calibration was based on a "Flux density" of 3C279 of 10 Jy and used 3C279 as bandpass calibrator.
3) After an initial calibration based on 3C279, the calibrators and 3C286 were self calibrated and the models used in subsequent calibration (although all were unresolved in this dataset).
4) A single scan on 3C279 was used to fix the Y/X gains and subsequent calibration averaged the parallel hands before determining calibration.
5) The calibrators and 3C286 were then used to determine short period phase fluctuations,
6) followed by scan averaged amplitude and phase corrections.
7) A single scan of 3C279 was used to correct the X-Y delays.
8) Data had calibration applied using Obit task Splat.
9) Polarization calibration used 3C279, J1337-1257, and J131029+322051 solving for the source polarization, Y/X gains and X-Y phases. Since only the target (3C286) had a known polarization angle the feed orientation were left at the nominal values. Solutions were performed in blocks of 250 MHz.
10) Y data from antenna 22 were found to be unreliable and were excluded from further analysis.

After calibration, the data were imaged using Obit task Imager using short period phase self calibration followed by scan averaged amplitude and phase self calibration. As all sources were unresolved, the value in the Stokes I, Q, U

TABLE II
Image RMS

Source	Day	I rms mJy/bm	Q rms mJy/bm	U rms mJy/bm	V rms mJy/bm
3C286	1	33	3.8	3.0	2.2
3C138	1	27	8.6	13.4	2.5
B1934-638	1	0.8	0.8	0.9	0.6
ph cal	1	4.7	0.7	0.9	0.3
3C286	2	23	2.3	2.3	0.2
3C138	2	26	8.3	12.0	3.7
B1934-638	2	3.7	1.0	1.2	0.7
ph cal	2	5.0	0.8	1.1	0.4
3C286	3	20	7.0,	6.4	1.7
B1934-638	3	11	2.3	2.0	1.2
quasar	3	4.5	0.8	0.6	0.2

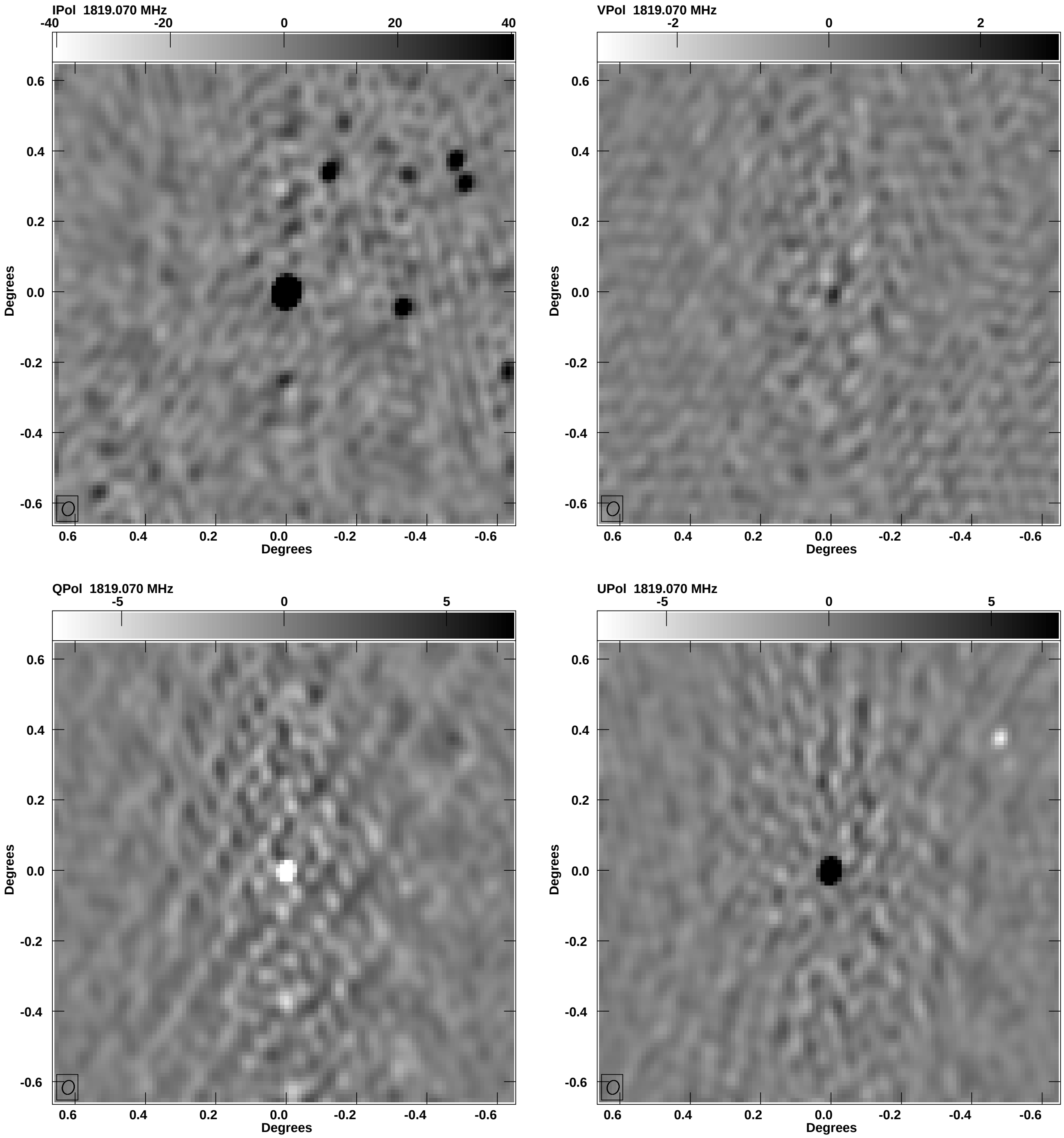

Fig. 1. Negative grayscale images of a quasar observed with KAT-7 in Stokes I (top left), V (top, right), Q (botton left) and U (bottom right). Intensity scale is given by the bar at the top labeled in mJy/beam. Maximum I is 2.71 Jy/beam, Q is -27 mJy/beam, U is 81 mJy/beam. CLEAN restoring beam is shown in the lower left.

TABLE III
Calibrator polarization

Source	I Jy/bm	frac. lin. pol	EVPA °
3C279	10.0	0.118	33.7
3C286	0.274	0.163	38.1
J1337-125	3.00	0.033	62.8
J131029+322051	0.636	0.048	85.8

and V images at the location of the calibrator were used for evaluation. Polarization results are given in Table I and the associated image's RMSes in Table II.

The images of 3C286 in various Stokes parameters are shown in Figure 2 and statistical measures in Tables III and IV. Images in Stokes I, Q and U show no significant artifacts while the respponse in Stokes V is clearly spurious, the source position is centered between the positive and negative responses and all calibrators show the same pattern at ± 0.4% of the Stokes I peak.

VIII. Discussion

A method of calibrating the polarized response from radio interferometer arrays using linearly polarized feeds is described and an implementation tested using data from the KAT-7 telescope. The results in the previous section show good repeatability of results for a number of sources and a low level of residual artifacts in the derived polarization images. The low level of polarized residuals in images of the very weakly polarized source B1934-638, less than 0.1%, are indicative of the quality of correction. Polarized emission is even visible from a weaker source in the field shown in Figure 1.

A calibrator of known EVPA is needed to accurately determine the orientations of the feeds in order to ensure accurate measures of the angle of linear polarization (EVPA). This was done in the cases of the KAT-7 data tests described above. However, after calibration there were residual errors in EVPA. Polarization models are given in [9] for 3C138 (7.5% EVPA=-11°) and 3C286 (9.5% , EVPA=33°) at 1.45 GHz. 3C286 was used to set the EVPA scale but the results shown in Table I all gave an EVLA of ∼30°, 3° lower than the value used in the calibration of ∼33°. The EVPA values for 3C138 given in Table I are about 10° lower than the value given by [9]. The fractional linear polarizations given in Table I are in good agreement with [9]. The reasons for the discrepancy in EVPA, and in particular, the differences for 3C138 and 3C286 are unclear.

The ALMA example analysis gave a fractional polarization of 16.3% and an EVPA of 38.1°. This is in reasonable agreement with other measurements [10] and shows the efficacy of using the nominal ALMA feed orientations. The reasons for the clearly spurious Stokes V image of 3C286 is not understood.

TABLE IV
Image RMS

Source	I rms mJy/bm	Q rms mJy/bm	U rms mJy/bm	V rms mJy/bm
3C279	267	12	29	2.0
3C286	8.4	0.1	1.4	0.1
J1337-125	76	0.3	0.2	0.5
J131029+322051	20	0.1	0.1	0.1

Acknowledgment

I thank Rick Perley for providing his analysis of radio interferometric polarimetry. I would also like to thank Tom Maunch and Nadeem Oozeer of SKA/SA for providing KAT-7 test data and to Paulo Cortes for providing the ALMA test dataset.

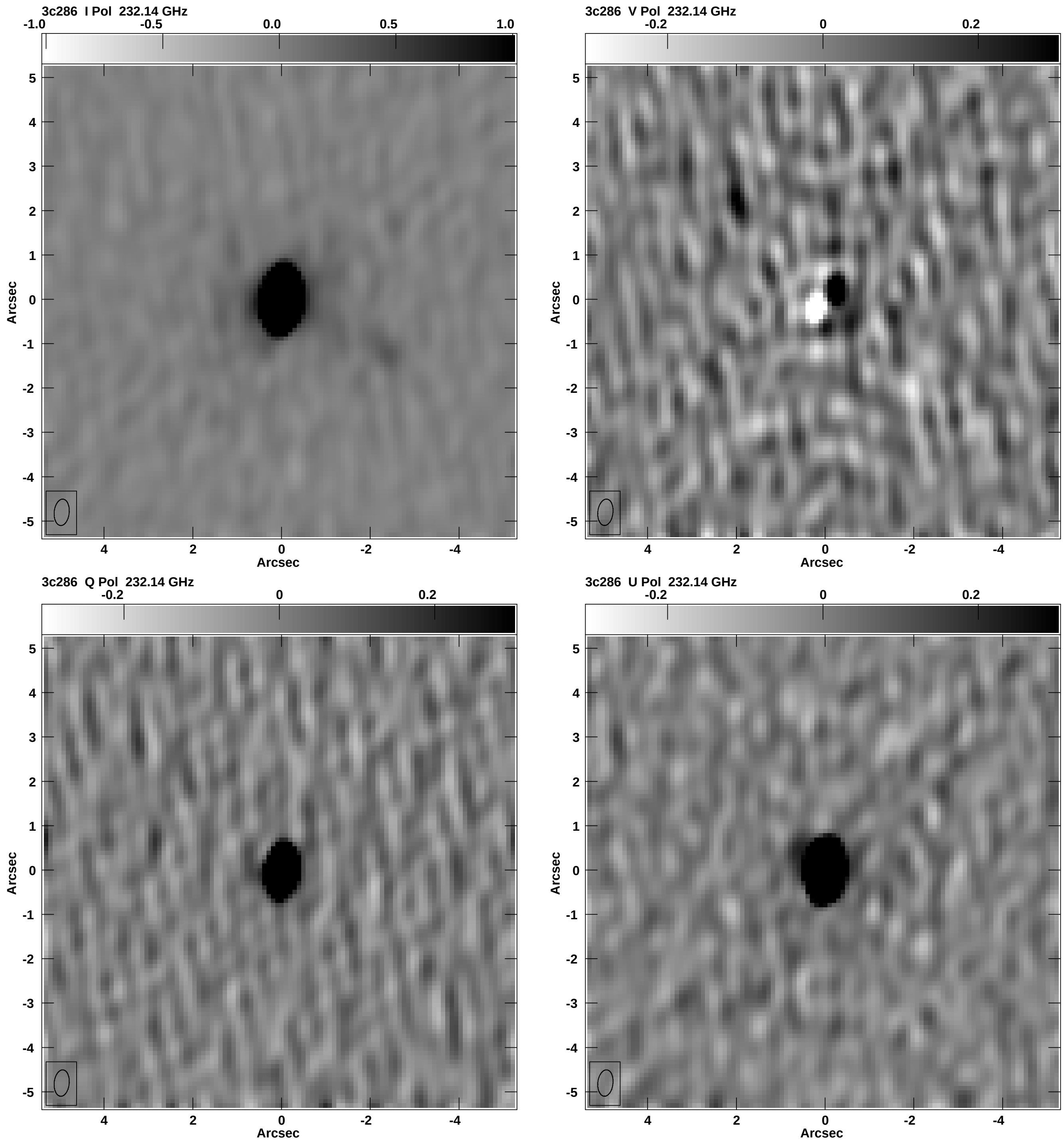

Fig. 2. Negative grayscale images of 3c286 observed by ALMA in Stokes I (top left), V (top, right), Q (botton left) and U (bottom right). Intensity scale is given by the bar at the top labeled in mJy/beam. CLEAN restoring beam is shown in the lower left.

APPENDIX

Muller matrix

A polarization Jones matrix which includes the effects of parallel–hand calibration can be constructed for each antenna:

$$\mathbf{J} = \begin{vmatrix} g_X cos(\frac{\pi}{4}+\theta_X)e^{-j(\phi_X)} & g_X sin(\frac{\pi}{4}+\theta_X)e^{j(\phi_X)} \\ g_Y sin(\frac{\pi}{4}-\theta_Y)e^{j(\phi_Y)} & g_Y cos(\frac{\pi}{4}-\theta_Y)e^{-j(\phi_Y)} \end{vmatrix}$$

where θ is the ellipticity, ϕ the orientation, j is $\sqrt{-1}$, g_X and g_Y are corrections to the gains of the X and Y feeds resulting from the parallel hand calibration, The Muller matrix, M_{ik}, for baseline i-k is then the outer product of $\mathbf{J}_i$ and $\mathbf{J}^*_k$.

$$\mathbf{M}_{ik} \;=\; \mathbf{J}_i \;\otimes \mathbf{J}^*_k$$

In order to efficiently compute the Muller matrices, for each antenna i, define:

$$\begin{aligned} C_{X,i} =& \;\; cos(\frac{\pi}{4}+\theta_{X,i})\; e^{-j\phi_{X,i}} \\ C_{Y,i} =& \;\; cos(\frac{\pi}{4}-\theta_{Y,i})\; e^{j(\phi_{Y,i})} \\ S_{X,i} =& \;\; sin(\frac{\pi}{4}+\theta_{X,i})\; e^{j\phi_{X,i}} \\ S_{Y,i} =& \;\; sin(\frac{\pi}{4}-\theta_{Y,i})\; e^{-j(\phi_{Y,i})} \end{aligned}$$

and for each baseline $i-k$ define:

$$\begin{aligned} \Delta\chi_{ik} &= e^{j(\chi_i - \chi_k)} \\ \Sigma\chi_{ik} &= e^{j(\chi_i + \chi_k)} \end{aligned}$$

The Jones matrix then becomes:

$$\mathbf{J} = \begin{vmatrix} C_{X,i} & S_{X,i} \\ S_{Y,i} & C_{Y,i} \end{vmatrix}$$

The elements of the Muller matrix to convert the circular basis model visibility to the corrupted linear basis visibilities is:

$$\mathbf{M_{ik}} = \begin{vmatrix} C_{X,i}C^*_{X,k} & C_{X,i}S^*_{X,k} & S_{X,i}C^*_{X,k} & S_{X,i}S^*_{X,k} \\ C_{X,i}S^*_{Y,k} & C_{X,i}C^*_{Y,k} & S_{X,i}S^*_{Y,k} & S_{X,i}C^*_{Y,k} \\ S_{Y,i}C^*_{X,k} & S_{Y,i}S^*_{X,k} & C_{Y,i}C^*_{X,k} & C_{Y,i}S^*_{X,k} \\ S_{Y,i}S^*_{Y,k} & S_{Y,i}C^*_{Y,k} & C_{Y,i}S^*_{Y,k} & C_{Y,i}C^*_{Y,k} \end{vmatrix}$$

where * denotes the complex conjugate.

The model visibility is given by:

$$\mathbf{S_C} = \begin{vmatrix} ipol + vpol \\ qpol + j\;\, upol \\ qpol - j\;\, upol \\ ipol - vpol \end{vmatrix}$$

where $ipol$, $qpol$, $upol$ and $vpol$ are the Stokes' I, Q, U and V of the source.

Applying corrections for the parallactic angle:

$$\mathbf{S} = \mathbf{S_C} \begin{vmatrix} \Delta\chi^*_{ik} & 0 & 0 & 0 \\ 0 & \Sigma\chi^*_{ik} & 0 & 0 \\ 0 & 0 & \Sigma\chi_{ik} & 0 \\ 0 & 0 & 0 & \Delta\chi_{ik} \end{vmatrix}$$

The corrections to the parallel hand calibration can be described as

$$\mathbf{C_{ik}} = \begin{vmatrix} g_{x,i}g_{x,k} \\ g_{x,i}g_{y,k}e^{j\delta} \\ g_{y,i}g_{x,k}e^{-j\delta} \\ g_{x,i}g_{x,k} \end{vmatrix}$$

The model of the observed visibility is then

$$\mathbf{V}_{model\,ik} \;=\; \mathbf{M}_{ik}\;\mathbf{S}\;\mathbf{C_{ik}} \tag{6}$$

The components of the model visibility vector in the linear basis, $\mathbf{V}_{model\,ik}$, are:

$$\begin{aligned} V_{XX_{ik}} &= (S_0 M_{0,0} + S_1 M_{0,1} + S_2 M_{0,2} + S_3 M_{0,3}) g_{X,i} g_{X,k} \\ V_{XY_{ik}} &= (S_0 M_{1,0} + S_1 M_{1,1} + S_2 M_{1,2} + S_3 M_{1,3}) g_{X,i} g_{Y,k} e^{i\delta} \\ V_{YX_{ik}} &= (S_0 M_{2,0} + S_1 M_{2,1} + S_2 M_{2,2} + S_3 M_{2,3}) g_{Y,i} g_{X,k} e^{-i\delta} \\ V_{YY_{ik}} &= (S_0 M_{3,0} + S_1 M_{3,1} + S_2 M_{3,2} + S_3 M_{3,3}) g_{Y,i} g_{Y,k} \end{aligned} \tag{7}$$

Partial derivatives

The nonlinear fitting routines need the first and second partial derivatives of Eq. 7 wrt each of the parameters being fitted. The parameters which may be adjusted and for which partial derivatives may be needed are:

- $ipol$ Source Stokes I.
- $qpol$ Source Stokes Q.
- $upol$ Source Stokes U.
- $vpol$ Source Stokes V.
- ϕ_{X_i} Orientation of X feed antenna i.
- ϕ_{Y_i} Orientation of Y feed antenna i.
- θ_{X_i} Ellipticity of X feed antenna i.
- θ_{Y_i} Ellipticity of Y feed antenna i.
- g_{X_i} Gain correction to X feed antenna i.
- g_{Y_i} Gain correction to Y feed antenna i.
- δ Phase difference between X and Y parallel systems.

Source derivatives, all second derivatives are 0.

$$\begin{aligned} \frac{\partial V_{XX}}{\partial ipol} &= (\;\; C_{X,i}C^*_{X,k}\Delta^*\chi_{ik} + \;\; S_{X,i}S^*_{X,k}\Delta^{\chi}_{ik})g_{X,i}g_{X,k} \\ &= (\;\; M_{0,0}\Delta^*\chi_{ik} + \;\; M_{0,3}\Delta^{\chi}_{ik})g_{X,i}g_{X,k} \\ \frac{\partial V_{XX}}{\partial qpol} &= (\;\; C_{X,i}S^*_{X,k}\Sigma^*\chi_{ik} + \;\; S_{X,i}C^*_{X,k}\Sigma^{\chi}_{ik})g_{X,i}g_{X,k} \\ &= (\;\; M_{0,1}\Sigma^*\chi_{ik} + \;\; M_{0,2}\Sigma^{\chi}_{ik})g_{X,i}g_{X,k} \\ \frac{\partial V_{XX}}{\partial upol} &= (j\;\, C_{X,i}S^*_{X,k}\Sigma^*\chi_{ik} - j\;\, S_{X,i}C^*_{X,k}\Sigma^{\chi}_{ik})g_{X,i}g_{X,k} \\ &= (j\;\, M_{0,1}\Sigma^*\chi_{ik} - j\;\, M_{0,2}\Sigma^{\chi}_{ik})g_{X,i}g_{X,k} \\ \frac{\partial V_{XX}}{\partial vpol} &= (\;\; C_{X,i}C^*_{X,k}\Delta^*\chi_{ik} - \;\; S_{X,i}S^*_{X,k}\Delta^{\chi}_{ik})g_{X,i}g_{X,k} \\ &= (\;\; M_{0,0}\Delta^*\chi_{ik} - \;\; M_{0,3}\Delta^{\chi}_{ik})g_{X,i}g_{X,k} \end{aligned}$$

$$\begin{aligned} \frac{\partial V_{YY}}{\partial ipol} &= (\;\; S_{Y,i}S^*_{Y,k}\Delta^*\chi_{ik} + \;\; C_{Y,i}C^*_{Y,k}\Delta^{\chi}_{ik})g_{Y,i}g_{Y,k} \\ &= (\;\; M_{3,0}\Delta^*\chi_{ik} + \;\; M_{3,3}\Delta^{\chi}_{ik})g_{Y,i}g_{Y,k} \\ \frac{\partial V_{YY}}{\partial qpol} &= (\;\; S_{Y,i}C^*_{Y,k}\Sigma^*\chi_{ik} + \;\; C_{Y,i}S^*_{Y,k}\Sigma^{\chi}_{ik})g_{Y,i}g_{Y,k} \\ &= (\;\; M_{3,1}\Sigma^*\chi_{ik} + \;\; M_{3,2}\Sigma^{\chi}_{ik})g_{Y,i}g_{Y,k} \\ \frac{\partial V_{YY}}{\partial upol} &= (j\;\, S_{Y,i}C^*_{Y,k}\Sigma^*\chi_{ik} - j\;\, C_{Y,i}S^*_{Y,k}\Sigma^{\chi}_{ik})g_{Y,i}g_{Y,k} \\ &= (j\;\, M_{3,1}\Sigma^*\chi_{ik} - j\;\, M_{3,2}\Sigma^{\chi}_{ik})g_{Y,i}g_{Y,k} \\ \frac{\partial V_{YY}}{\partial vpol} &= (\;\; S_{Y,i}S^*_{Y,k}\Delta^*\chi_{ik} - \;\; C_{Y,i}C^*_{Y,k}\Delta^{\chi}_{ik})g_{Y,i}g_{Y,k} \\ &= (\;\; M_{3,0}\Delta^*\chi_{ik} + - \;\; M_{3,3}\Delta^{\chi}_{ik})g_{Y,i}g_{Y,k} \end{aligned}$$

$$\frac{\partial V_{XY}}{\partial ipol} = (\quad C_{X,i}S^*_{Y,k}\Delta^*\chi_{ik} + \quad S_{X,i}C^*_{Y,k}\Delta^\chi_{ik})g_{X,i}g_{Y,k}e^{j\delta}$$
$$= (\quad M_{1,0}\Delta^*\chi_{ik} + \quad M_{1,3}\Delta^\chi_{ik})g_{X,i}g_{Y,k}e^{j\delta}$$
$$\frac{\partial V_{XY}}{\partial qpol} = (\quad C_{X,i}C^*_{Y,k}\Sigma^*\chi_{ik} + \quad S_{X,i}S^*_{Y,k}\Sigma^\chi_{ik})g_{X,i}g_{Y,k}e^{j\delta}$$
$$= (\quad M_{1,1}\Sigma^*\chi_{ik} + \quad M_{1,2}\Sigma^\chi_{ik})g_{X,i}g_{Y,k}e^{j\delta}$$
$$\frac{\partial V_{XY}}{\partial upol} = (j \ C_{X,i}C^*_{Y,k}\Sigma^*\chi_{ik} - j \ S_{X,i}S^*_{Y,k}\Sigma^\chi_{ik})g_{X,i}g_{Y,k}e^{j\delta}$$
$$= (j \ M_{1,1}\Sigma^*\chi_{ik} - j \ M_{1,2}\Sigma^\chi_{ik})g_{X,i}g_{Y,k}e^{j\delta}$$
$$\frac{\partial V_{XY}}{\partial vpol} = (\quad C_{X,i}S^*_{Y,k}\Delta^*\chi_{ik} - \quad S_{X,i}C^*_{Y,k}\Delta^\chi_{ik})g_{X,i}g_{Y,k}e^{j\delta}$$
$$= (\quad M_{1,0}\Delta^*\chi_{ik} - \quad M_{1,3}\Delta^\chi_{ik})g_{X,i}g_{Y,k}e^{j\delta}$$
$$\frac{\partial V_{YX}}{\partial ipol} = (\quad S_{Y,i}C^*_{X,k}\Delta^*\chi_{ik} + \quad C_{Y,i}S^*_{X,k}\Delta^\chi_{ik})g_{Y,i}g_{X,k}e^{-j\delta}$$
$$= (\quad M_{2,0}\Delta^*\chi_{ik} + \quad M_{2,3}\Delta^\chi_{ik})g_{Y,i}g_{X,k}e^{-j\delta}$$
$$\frac{\partial V_{YX}}{\partial qpol} = (\quad S_{Y,i}S^*_{X,k}\Sigma^*\chi_{ik} + \quad C_{Y,i}C^*_{X,k}\Sigma^\chi_{ik})g_{Y,i}g_{X,k}e^{-j\delta}$$
$$= (\quad M_{2,1}\Sigma^*\chi_{ik} + \quad M_{2,2}\Sigma^\chi_{ik})g_{Y,i}g_{X,k}e^{-j\delta}$$
$$\frac{\partial V_{YX}}{\partial upol} = (j \ S_{Y,i}S^*_{X,k}\Sigma^*\chi_{ik} - j \ C_{Y,i}C^*_{X,k}\Sigma^\chi_{ik})g_{Y,i}g_{X,k}e^{-j\delta}$$
$$= (j \ M_{2,1}\Sigma^*\chi_{ik} - j \ M_{2,2}\Sigma^\chi_{ik})g_{Y,i}g_{X,k}e^{-j\delta}$$
$$\frac{\partial V_{YX}}{\partial vpol} = (\quad S_{Y,i}C^*_{X,k}\Delta^*\chi_{ik} - \quad C_{Y,i}S^*_{X,k}\Delta^\chi_{ik})g_{Y,i}g_{X,k}e^{-j\delta}$$
$$= (\quad M_{2,0}\Delta^*\chi_{ik} - \quad M_{2,3}\Delta^\chi_{ik})g_{Y,i}g_{X,k}e^{-j\delta}$$

Non zero derivatives in ϕ_X:

$$\frac{\partial V_{XX}}{\partial \phi_{X_i}} = (- jS_0M_{0,0} - jS_1M_{0,1} + jS_2M_{0,2} + jS_3M_{0,3}) g_{X_i}g_{X_k}$$
$$\frac{\partial^2 V_{XX}}{\partial \phi^2_{X_i}} = - V_{XX}$$
$$\frac{\partial V_{XX}}{\partial \phi_{X_k}} = (+ jS_0M_{0,0} - jS_1M_{0,1} + jS_2M_{0,2} - jS_3M_{0,3}) g_{X_i}g_{X_k}$$
$$\frac{\partial^2 V_{XX}}{\partial \phi^2_{X_i}} = - V_{XX}$$
$$\frac{\partial V_{XY}}{\partial \phi_{X_i}} = (- jS_0M_{1,0} - jS_1M_{1,1} + jS_2M_{1,2} + jS_3M_{1,3}) g_{X_i}g_{Y_k}e^{j\delta}$$
$$\frac{\partial^2 V_{XY}}{\partial \phi^2_{X_i}} = - V_{XY}$$
$$\frac{\partial V_{YX}}{\partial \phi_{X_k}} = (+ jS_0M_{2,0} - jS_1M_{2,1} + jS_2M_{2,2} - jS_3M_{2,3}) g_{Y_i}g_{X_k}e^{-j\delta}$$
$$\frac{\partial^2 V_{YX}}{\partial \phi^2_{X_k}} = - V_{YX}$$

Non zero derivatives wrt ϕ_Y:

$$\frac{\partial V_{XY}}{\partial \phi_{Y_k}} = (+ jS_0M_{1,0} - jS_1M_{1,1} + jS_2M_{1,2} - jS_3M_{1,3}) g_{X_i}g_{Y_k}e^{j\delta}$$
$$\frac{\partial^2 V_{XY}}{\partial \phi^2_{Y_k}} = - V_{XY}$$
$$\frac{\partial V_{YX}}{\partial \phi_{Y_i}} = (- jS_0M_{2,0} - jS_1M_{2,1} + jS_2M_{2,2} + jS_3M_{2,3}) g_{Y_i}g_{X_k}e^{-j\delta}$$
$$\frac{\partial^2 V_{YX}}{\partial \phi^2_{Y_i}} = - V_{YX}$$
$$\frac{\partial V_{YY}}{\partial \phi_{Y_i}} = (- jS_0M_{3,0} - jS_1M_{3,1} + jS_2M_{3,2} + jS_3M_{3,3}) g_{Y_i}g_{Y_k}$$
$$\frac{\partial^2 V_{YY}}{\partial \phi^2_{Y_i}} = - V_{YY}$$
$$\frac{\partial V_{YY}}{\partial \phi_{Y_k}} = (+ jS_0M_{3,0} - jS_1M_{3,1} + jS_2M_{3,2} - jS_3M_{3,3}) g_{Y_i}g_{Y_k}$$
$$\frac{\partial^2 V_{YY}}{\partial \phi^2_{Y_k}} = - V_{YY}$$

Non zero derivatives wrt θ_X:

$$\frac{\partial V_{XX}}{\partial \theta_{X_i}} = j(-S_0CX^*_kSX^*_i - S_1SX^*_kSX^*_i + S_2CX^*_kCX^*_i + S_3SX^*_kCX^*_i) g_{X_i}g_{X_k}$$
$$\frac{\partial^2 V_{XX}}{\partial \theta^2_{X_i}} = - V_{XX}$$
$$\frac{\partial V_{XX}}{\partial \theta_{X_k}} = j(-S_0CX_i\Delta\chi^*_{ik}SX_k + S_1CX_i\Sigma\chi^*_{ik}CX_k - S_2SX_i\Sigma\chi_{ik}SX_k + S_3SX_i\Delta\chi_{ik}CX_k) g_{X_i}g_{X_k}$$
$$\frac{\partial^2 V_{XX}}{\partial \theta^2_{X_k}} = - V_{XX}$$
$$\frac{\partial V_{XY}}{\partial \theta_{X_i}} = j(-S_0SY^*_kSX^*_i - S_1CY^*_kSX^*_i + S_2SY^*_kCX^*_i + S_3CY^*_kCX^*_i) g_{X_i}g_{X_k}e^{j\delta}$$
$$\frac{\partial^2 V_{XY}}{\partial \theta^2_{X_i}} = - V_{XY}$$

$$\frac{\partial V_{YX}}{\partial \theta_{X_k}} = j(-S_0 SY_i^* SX_k + S_1 SY_i^* CX_k - S_2 CY_i^* SX_k + S_3 CY_i^* CX_k) g_{X_i} g_{X_k} e^{-j\delta}$$

$$\frac{\partial^2 V_{YX}}{\partial \theta_{X_k}^2} = -\ V_{YX}$$

Non zero derivatives wrt θ_Y:

$$\frac{\partial V_{YY}}{\partial \theta_{Y_i}} = j(-S_0 SY_k^* CY_i^* - S_1 CY_k^* CY_i^* + S_2 SY_k^* SY_i^* + S_3 CY_k^* SY_i^*) g_{Y_i} g_{Y_k}$$

$$\frac{\partial^2 V_{YY}}{\partial \theta_{Y_i}^2} = -\ V_{YY}$$

$$\frac{\partial V_{YY}}{\partial \theta_{Y_k}} = j - (S_0 SY_i CY_k + S_1 SY_i SY_k - S_2 CY_i CY_k + S_3 CY_i SY_k) g_{Y_i} g_{Y_k}$$

$$\frac{\partial^2 V_{YY}}{\partial \theta_{Y_k}^2} = -\ V_{YY}$$

$$\frac{\partial V_{XY}}{\partial \theta_{Y_k}} = j(-S_0 CX_i CY_k + S_1 CX_i SY_k - S_2 SX_i CY_k + S_3 SX_i SY_k) g_{X_i} g_{Y_k} e^{j\delta}$$

$$\frac{\partial^2 V_{XY}}{\partial \theta_{Y_k}^2} = -\ V_{XY}$$

$$\frac{\partial V_{YX}}{\partial \theta_{Y_i}} = j(-S_0 CX_k^* CY_i^* - S_1 SX_k^* CY_i^* + S_2 CX_k^* SY_i^* + S_3 SX_k^* SY_i^*) g_{Y_i} g_{X_k} e^{-j\delta}$$

$$\frac{\partial^2 V_{YX}}{\partial \theta_{Y_i}^2} = -\ V_{YY}$$

Derivatives wrt g_X, second derivatives are 0.0:

$$\frac{\partial V_{XX}}{\partial g_{x,i}} = (S_0 M_{0,0} + S_1 M_{0,1} + S_2 M_{0,2} + S_3 M_{0,3}) g_{x,k}$$
$$\frac{\partial V_{XX}}{\partial g_{x,k}} = (S_0 M_{1,0} + S_1 M_{1,1} + S_2 M_{1,2} + S_3 M_{1,3}) g_{x,i}$$
$$\frac{\partial V_{XY}}{\partial g_{x,i}} = (S_0 M_{2,0} + S_1 M_{2,1} + S_2 M_{2,2} + S_3 M_{2,3}) g_{Y,k} e^{i\delta}$$
$$\frac{\partial V_{YX}}{\partial g_{x,k}} = (S_0 M_{3,0} + S_1 M_{3,1} + S_2 M_{3,2} + S_3 M_{3,3}) g_{Y,i} e^{-i\delta}$$

Derivatives wrt g_Y, second derivatives are 0.0:

$$\frac{\partial V_{XY}}{\partial g_{Y,k}} = (S_0 M_{0,0} + S_1 M_{0,1} + S_2 M_{0,2} + S_3 M_{0,3}) g_{x,i} e^{i\delta}$$
$$\frac{\partial V_{YX}}{\partial g_{Y,i}} = (S_0 M_{1,0} + S_1 M_{1,1} + S_2 M_{1,2} + S_3 M_{1,3}) g_{x,k} e^{-i\delta}$$
$$\frac{\partial V_{YY}}{\partial g_{Y,i}} = (S_0 M_{2,0} + S_1 M_{2,1} + S_2 M_{2,2} + S_3 M_{2,3}) g_{Y,k}$$
$$\frac{\partial V_{YY}}{\partial g_{Y,k}} = (S_0 M_{3,0} + S_1 M_{3,1} + S_2 M_{3,2} + S_3 M_{3,3}) g_{Y,i}$$

Non zero derivatives in δ:

$$\frac{\partial V_{XY}}{\partial \delta} = +\ j\ V_{V_{YX}}, \qquad \frac{\partial^2 V_{XY}}{\partial \delta^2} = +\ j\ \frac{\partial V_{XY}}{\partial \delta}$$
$$\frac{\partial V_{YX}}{\partial \delta} = -\ j\ V_{XY}, \qquad \frac{\partial^2 V_{YX}}{\partial \delta^2} = -\ j\ \frac{\partial V_{YX}}{\partial \delta}$$

Derivatives of χ^2 wrt parameters

The χ^2 of the fit is defined as

$$\chi^2 = \sum_{i=0}^{n} (model_i - obs_i)^2 / \sigma_i^2$$

where $model_i$ is the model value for observation i (real or imaginary part of visibility), obs_i is the observation for i and σ_i^2 is the variance of the amplitude of observation i. Denote $model_i - obs_i$ as $resid_i$.

The derivative of χ^2 wrt each parameter p is:

$$\frac{\partial \chi^2}{\partial p} = \sum_{i=0}^{n} 2\ \left(resid_i \frac{\partial model_i}{\partial p}\right) / \sigma_i^2$$

This expression is complex, to get the real value, instead use

$$\frac{\partial \chi^2}{\partial p} = \sum_{i=0}^{n} 2\ \Big(\mathrm{Real}(resid_i)\mathrm{Real}(\frac{\partial model_i}{\partial p}) + \mathrm{Imag}(resid_i)\mathrm{Imag}(\frac{\partial model_i}{\partial p})\Big) / \sigma_i^2$$

where Real and Imag denote the real and imaginary parts of the argument.

The second derivative of χ^2 wrt each parameter p is:

$$\frac{\partial^2 \chi^2}{\partial p^2} = \sum_{i=0}^{n} 2\ \left(\frac{\partial model_i}{\partial p}\frac{\partial model_i}{\partial p} + resid_i \frac{\partial^2 model_i}{\partial p^2}\right) / \sigma_i^2$$

This expression is also complex, to get the real value, instead use

$$\frac{\partial^2 \chi^2}{\partial p^2} = \sum_{i=0}^{n} 2\ \Big(\mathrm{Real}(\frac{\partial model_i}{\partial p})\mathrm{Real}(\frac{\partial model_i}{\partial p}) + \mathrm{Imag}(\frac{\partial model_i}{\partial p}\mathrm{Imag}(\frac{\partial model_i}{\partial p}) + \mathrm{Real}(resid_i)\mathrm{Real}(\frac{\partial^2 model_i}{\partial p^2}) + \mathrm{Imag}(resid_i)\mathrm{Imag}(\frac{\partial^2 model_i}{\partial p^2}))\Big) / \sigma_i^2$$

REFERENCES

[1] W. D. Cotton, "Obit: A Development Environment for Astronomical Algorithms," *PASP*, vol. 120, pp. 439–448, 2008.

[2] W. D. Cotton, "On–axis Instrumental Polarization Calibration for Circular Feeds," *Obit Development Memo Series*, vol. 30, pp. 1–14, 2012.

[3] R. A. Perley, "Polarimetry 101 for the EVLA," *privte communication*, 2010.

[4] A. R. Thompson, J. M. Moran, and G. W. Swenson, Jr., *Interferometry and Synthesis in Radio Astronomy, 2nd Edition*, Thompson, A. R., Moran, J. M., & Swenson, G. W., Jr., Ed. Wiley-Interscience, 2001.

[5] W. D. Cotton, "Polarization in Interferometry," in *Synthesis Imaging in Radio Astronomy II*, ser. Astronomical Society of the Pacific Conference Series, G. B. Taylor, C. L. Carilli, and R. A. Perley, Eds., vol. 180, 1999, pp. 111–+.

[6] R. J. Sault, J. P. Hamaker, and J. D. Bregman, "Understanding radio polarimetry. II. Instrumental calibration of an interferometer array." *A&A Suppl.*, vol. 117, pp. 149–+, 1996.

[7] W. D. Cotton, "A New Method for Cross Polarized Delay Calibration of Radio Interferometers," *JAI*, vol. 1, p. 50001, 2012.

[8] R. J. Sault, N. E. B. Killeen, and M. J. Kesteven, "AT Polarization Calibration," *AT Memo series*, vol. AT 39.3/015, pp. 1–12, 1991.

[9] R. A. Perley and B. J. Butler, ""Integrated Polarization Properties of 3C48, 3C138, 3C147 and 3C286"," *AP J Supl.*, vol. 206, p. 16P, 2013.

[10] I. Agudo and et al., "3C286: a bright, compact, stable and highly polarized calibrator for millimeter-wavelength observations." *A&A*, vol. 541, pp. 111–+, 2012.